# Analysis of the apoptotic and therapeutic activities of histone deacetylase inhibitors by using a mouse model of B cell lymphoma

R. K. Lindemann*, A. Newbold*, K. F. Whitecross*, L. A. Cluse*, A. J. Frew*, L. Ellis*, S. Williams*, A. P. Wiegmans*, A. E. Dear†, C. L. Scott‡§, M. Pellegrini§, A. Wei§, V. M. Richon¶, Paul A. Marks‖**, S. W. Lowe‡, M. J. Smyth*††, and R. W. Johnstone*,**††

*Cancer Immunology Program, The Peter MacCallum Cancer Institute, Trescowthick Research Laboratories, St. Andrews Place, East Melbourne, Victoria 3002, Australia; †Australian Centre for Blood Diseases, Monash University, 6th Floor, Burnet Building, Prahran, Melbourne, Victoria 3181, Australia; ‡Cold Spring Harbor Laboratory, Cold Spring Harbor, NY 11724; §The Walter and Eliza Hall Institute, Melbourne, Victoria 3050, Australia; ‖Memorial Sloan–Kettering Cancer Center, New York, NY 10021; ¶Merck & Co., 33 Avenue Louis Pasteur, Boston, MA 02115; and ††Department of Pathology, University of Melbourne, Parkville, Victoria 3054, Australia

Contributed by Paul A. Marks, March 14, 2007 (sent for review January 25, 2007)

**Histone deacetylase inhibitors (HDACi) can elicit a range of biological responses that affect tumor growth and survival, including inhibition of cell cycle progression, induction of tumor cell-selective apoptosis, suppression of angiogenesis, and modulation of immune responses, and show promising activity against hematological malignancies in clinical trials. Using the Eμ-myc model of B cell lymphoma, we screened tumors with defined genetic alterations in apoptotic pathways for therapeutic responsiveness to the HDACi vorinostat. We demonstrated a direct correlation between induction of tumor cell apoptosis *in vivo* and therapeutic efficacy. Vorinostat did not require p53 activity or a functional death receptor pathway to kill Eμ-myc lymphomas and mediate a therapeutic response but depended on activation of the intrinsic apoptotic pathway with the proapoptotic BH3-only proteins Bid and Bim playing an important role. Our studies provide important information regarding the mechanisms of action of HDACi that have broad implications regarding stratification of patients receiving HDACi therapy alone or in combination with other anticancer agents.**

BH3-only proteins | Bid | Bim | vorinostat

Histone deacetylase inhibitors (HDACi) are a class of anticancer agents currently being tested as therapies for hematological malignancies and solid tumors (1). The anticancer activities of these agents may involve one or more biological effects, including induction of tumor cell differentiation, inhibition of angiogenesis, modulation of immune responses, and apoptosis (2). Transformed cell lines may respond to HDACi by undergoing apoptosis accompanied by cleavage and activation of the proapoptotic Bcl-2 family member Bid, loss of mitochondrial outer membrane potential (MOMP, $\Delta\psi_m$), reactive oxygen species (ROS) production, cytochrome *c* release, caspase activation, and DNA fragmentation (3–7). Overexpression of antiapoptotic Bcl-2 inhibited HDACi-induced apoptosis *in vitro*, indicating an important role for the mitochondrial apoptotic pathway in the tumoricidal action of HDACi (4, 7, 8). A role for the extrinsic apoptotic pathway has been proposed on the basis of studies showing that various TNF receptors and their ligands are transcriptionally activated after HDACi treatment that correlates with HDACi-induced apoptosis (2, 9). The clinical relevance of data obtained from *in vitro* systems may be limited. It is not known whether the therapeutic effects of HDACi depend on their intrinsic effects on tumor cell growth and/or survival, their indirect effects (i.e., immune modulation, antiangiogenesis), or a combination of these effects.

The Eμ-myc model of B cell lymphoma has been successfully used to characterize *in vivo* responses to anticancer drugs (10, 11). A key feature of the model is that defined cancer genotypes can be created by crossing Eμ-myc mice with gene-targeted knockout mice, or by retrovirally transducing primary lymphomas to overexpress a gene of interest. Using this model, we performed a candidate screen to identify the apoptotic proteins and pathways necessary for HDACi activity. HDACi rapidly induced death of Eμ-myc lymphoma cells mediated by the intrinsic apoptotic process. When transplanted into mice, Eμ-myc lymphomas were sensitive to the HDAC inhibitor vorinostat [suberoylanilide hydroxamic acid (SAHA)] (12), leading to prolonged survival compared with control-treated mice. The efficacy of vorinostat against Eμ-myc lymphomas was p53-independent and did not require a functional death receptor apoptotic pathway. Eμ-myc lymphomas overexpressing Bcl-2 or Bcl-$X_L$ were resistant to vorinostat-induced apoptosis but still underwent a block in cell cycle progression at the $G_1$/S transition. Vorinostat conferred no therapeutic effect against Eμ-myc/Bcl-2 or Eμ-myc/Bcl-$X_L$ lymphomas, demonstrating a direct link between the ability of this agent to induce apoptosis and therapeutic outcome. Constraining the cellular apoptotic program by genetic targeting of the BH3-only proapoptotic proteins Bid or Bim impinged on *in vivo* sensitivity to vorinostat and suppressed the therapeutic effect of the compound. Thus, we have identified key apoptotic molecules that not only control sensitivity of lymphoma cells to HDACi in *in vivo* assays but also determine therapeutic outcome.

## Results

**Eμ-myc B Cell Lymphomas Are Sensitive to HDACi *in Vitro*.** Cultured Eμ-myc lymphoma cells were incubated with various concentrations of the HDACis vorinostat, oxamflatin, and depsipeptide over 20 h, and cell viability was assessed by trypan blue exclusion assays (Fig. 1*a*). The concentration of HDACi resulting in 70%

Author contributions: R.K.L., C.L.S., S.W.L., and R.W.J. designed research; R.K.L., A.N., K.F.W., L.A.C., A.J.F., L.E., S.W., and A.P.W. performed research; A.E.D., C.L.S., M.P., A.W., V.M.R., and S.W.L. contributed new reagents/analytic tools; R.K.L., V.M.R., P.A.M., M.J.S., and R.W.J. analyzed data; and R.K.L. and R.W.J. wrote the paper.

Conflict of interest statement: Memorial Sloan–Kettering Cancer Center and Columbia University jointly hold patents on hydroxamic-based polar compounds, including SAHA, that were exclusively licensed to Aton Pharma, Inc., a biotechnology company acquired by Merck, Inc., in April 2004. P.A.M. and V.M.R. were founders of Aton and have a financial interest in Merck's further development of SAHA (vorinostat).

Abbreviations: HDACi, histone deacetylase inhibitor; IVA, *in vivo* apoptosis assay; MOMP, mitochondrial outer membrane potential; PI, propidium iodide; SAHA, suberoylanilide hydroxamic acid; TRAIL, tumor necrosis factor-related apoptosis-inducing ligand.

**To whom correspondence may be addressed. E-mail: marksp@mskcc.org or ricky.johnstone@petermac.org.

This article contains supporting information online at www.pnas.org/cgi/content/full/0702294104/DC1.

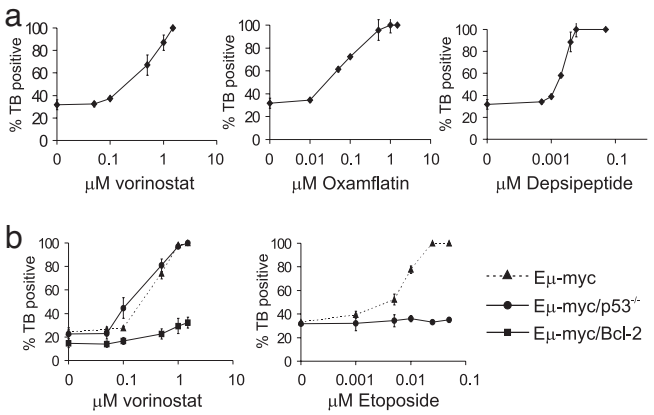


**Fig. 1.** *In vitro* sensitivity of Eμ-myc lymphomas to different HDACi. (*a*) Eμ-myc lymphomas were incubated with the indicated concentrations of vorinostat (*Left*), oxamflatin (*Center*), or depsipeptide (*Right*) for 20 h. (*b*) Eμ-myc, Eμ-myc/p53$^{-/-}$, and Eμ-myc/Bcl-2 lymphomas were incubated with increasing concentrations of vorinostat (*Left*), and Eμ-myc and Eμ-myc/p53$^{-/-}$ lymphomas were treated with increasing concentrations of Etoposide (*Right*) for 20 h. Cell viability was assessed by trypan blue uptake. Error bars indicate ±SEM of at least three independent experiments.

cell death ($IC_{70}$) was 0.5 μM for vorinostat, 0.1 μM for oxamflatin, and 3 nM for depsipeptide. All compounds induced comparable histone H3 hyperacetylation at their respective $IC_{70}$ concentrations (data not shown). Treatment of Eμ-myc lymphoma cells with HDACi at their $IC_{70}$ concentrations induced plasma membrane disruption, loss of MOMP, caspase activation, DNA fragmentation [supporting information (SI) Fig. 7], and annexin V staining (data not shown), indicating that HDACi induced apoptosis in Eμ-myc lymphomas.

We next tested the sensitivity of Eμ-myc lymphomas with defined defects in apoptotic pathways that confer resistance to anticancer drugs. The tumor-suppressor protein p53 plays a key role in mediating apoptosis by various cytotoxic agents (13), and hyperacetylation of p53 enhances the transcriptional activity of p53 (14, 15), resulting in increased expression of p53 target genes such as *Noxa* to initiate apoptosis (16). We tested the sensitivity of Eμ-myc/p53$^{-/-}$ lymphomas to vorinostat. Apoptotic signaling by HDACi was not impaired in the absence of p53 (Fig. 1*b* and SI Fig. 8). Eμ-myc/p53$^{-/-}$ lymphomas were also sensitive to oxamflatin and depsipeptide (data not shown) but are resistant to the alkylating agent Etoposide (Fig. 1*b*).

Using human tumor cell lines, we demonstrated that apoptotic activity of HDACi was inhibited by overexpression of Bcl-2 (3, 4). We developed Eμ-myc/Bcl-2 lymphoma cells and found that they were resistant to vorinostat-induced apoptosis (Fig. 1*b* and SI Fig. 8). These cells did undergo a $G_1$ cell cycle arrest (SI Fig. 8), with ≈69% of cells in $G_1$ after vorinostat treatment compared with ≈41% of vehicle-treated cells in $G_1$. Similar results were seen after treatment of Eμ-myc/Bcl-2 lymphomas with oxamflatin and depsipeptide (data not shown). $G_1$ cell cycle arrest of Eμ-myc/Bcl-2 lymphomas after HDACi treatment is consistent with the observed induction of *CDKN1A* encoding $p21^{WAF1/CIP1}$ in all Eμ-myc lymphomas that were studied (data not shown). Vorinostat-induced acetylation of histone H3 was equivalent in Eμ-myc, Eμ-myc/p53$^{-/-}$, and Eμ-myc/Bcl-2 lymphomas (SI Fig. 9).

**Vorinostat Has Antitumor Activity Against Eμ-myc Lymphomas *in Vivo*.** We next tested the ability of vorinostat to induce apoptosis *in vivo* and to prolong survival of lymphoma-bearing mice. Vorinostat induced a marked accumulation of Eμ-myc lymphomas displaying DNA fragmentation *in vivo* (Fig. 2*a*), comparable

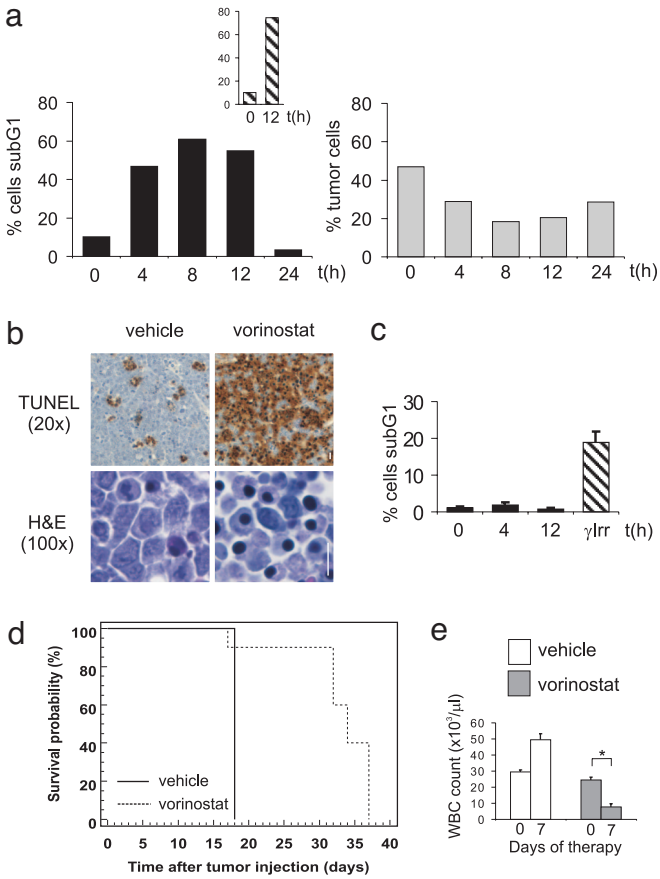


**Fig. 2.** Vorinostat selectively kills Eμ-myc lymphoma cells *in vivo*. (*a*) C57BL/6 mice bearing Eμ-myc lymphomas were injected with vorinostat (200 mg/kg i.p.) (*Left*) or 25 mg/kg i.p Etoposide (*Inset*), and lymphoma cells were harvested after the indicated time points. Apoptosis (sub-$G_1$ population) was measured by PI staining. (*Right*) The percentage of tumor cells in the lymph node of C57BL/6 mice bearing Eμ-myc lymphomas treated with vorinostat was determined by FACS analysis. (*b*) TUNEL (*Upper*) and H&E (*Lower*) staining of tissue sections from lymph nodes of mice bearing Eμ-myc lymphomas treated with vehicle (*Left*) or 200 mg/kg vorinostat (*Right*) for 12 h. (Scale bar: 10 μm.) (*c*) Apoptosis of splenocytes from vorinostat-treated or γ-irradiated mice (γ-Irr) (3 Gy) was assessed by PI staining. Error bars represent ±SEM from three independent experiments. (*d*) Eμ-myc lymphomas were transplanted into C57BL/6 mice, and treatment with vorinostat or vehicle commenced once WBC counts reached 13 × $10^3$ per microliter or greater (day 10) and were terminated on day 31. Kaplan–Meier survival curves of vehicle-treated mice (black line) and vorinostat-treated mice (dashed line) are shown. (*e*) WBC counts from mice transplanted with Eμ-myc lymphomas at the commencement of therapy (day = 0) with either vehicle or vorinostat or after 7 days of treatment (day = 7) are shown. Error bars represent ±SEM. *, $P < 0.05$.

to that seen with etoposide (Fig. 2*a Inset*). Similar to the *in vitro* data, vorinostat induced loss of MOMP and increased caspase activity in Eμ-myc lymphomas *in vivo* (data not shown). Vorinostat-induced apoptosis of Eμ-myc lymphoma cells *in vivo* was further assessed by TUNEL assay (17). In contrast to untreated controls, vorinostat-treatment resulted in a vast increase in apoptotic cells (Fig. 2*b Upper*) and large numbers of shrunken lymphoma cells displayed condensed chromatin (Fig. 2*b Lower*). Lymphocytes from vorinostat-treated C57BL/6 mice did not undergo apoptosis (Fig. 2*c*) indicating that vorinostat-induced apoptosis was selective for lymphoma cells and resulted in a decrease in Eμ-myc lymphoma cells from the lymph node (Fig. 2*a Lower*).

The survival of vorinostat-treated mice was significantly extended compared with vehicle-treated mice (Fig. 2*d*; median

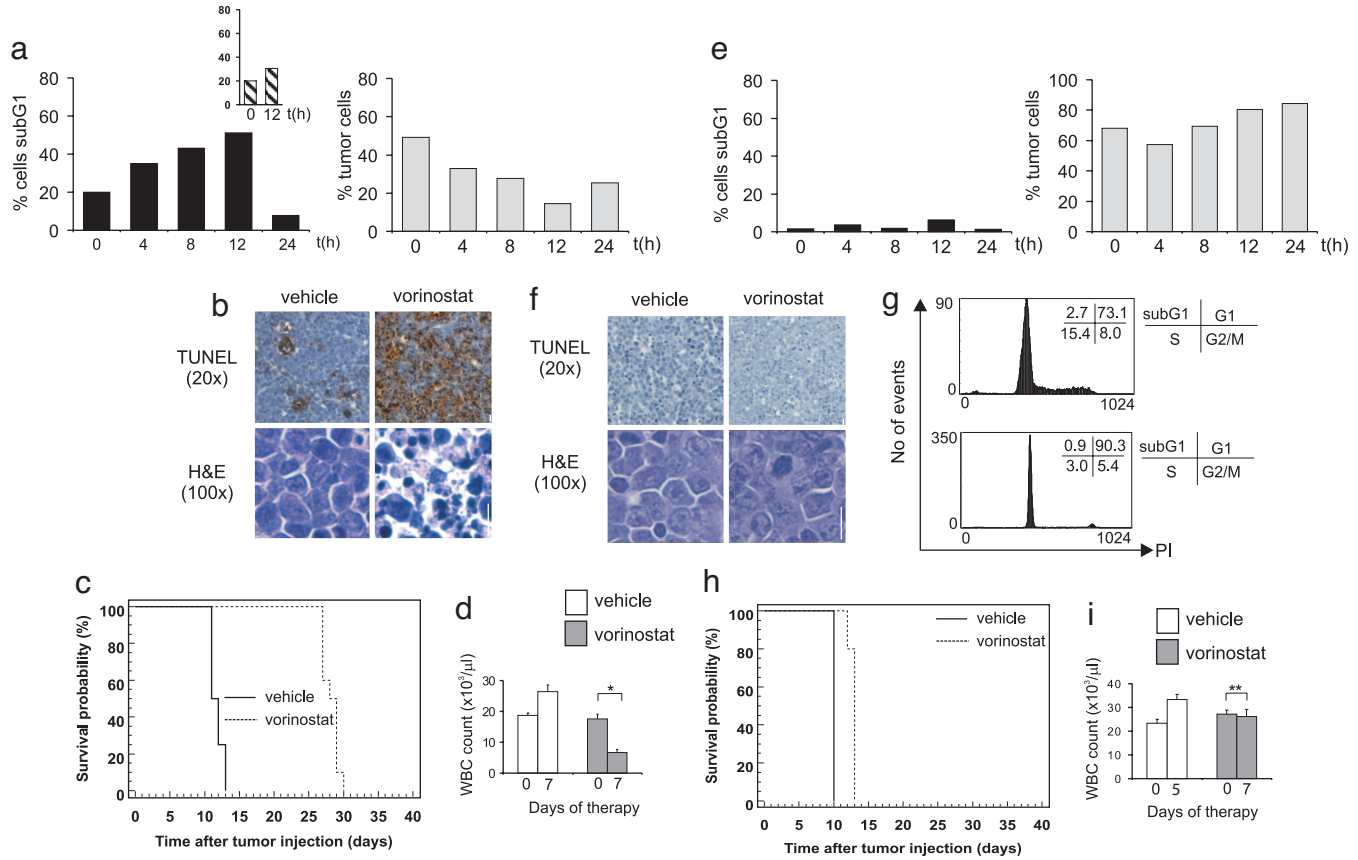


**Fig. 3.** Vorinostat therapy is p53-independent but completely inhibited by overexpression of Bcl-2. C57BL/6 mice were transplanted with E$\mu$-myc/p53$^{-/-}$ (*a–d*) or E$\mu$-myc/Bcl-2 (*e–i*) lymphomas. Vorinostat-induced apoptosis was assessed by PI staining/flow cytometry (IVA assay) (*a* and *e*) and by TUNEL assay and histological examination (*b* and *f*) as in Fig. 2. Vorinostat-mediated therapeutic responses (*c* and *h*) and effects on WBC counts (*d* and *i*) were performed as in Fig. 2. (*a Inset*) The percentage of sub-$G_1$ E$\mu$-myc/p53$^{-/-}$ lymphomas after 12-h treatment with Etoposide (25 mg/kg i.p.) is shown. (*c*) Treatment of E$\mu$-myc/p53$^{-/-}$ lymphomas commenced on day 10 after tumor injection and terminated on day 30. Kaplan–Meier survival curves of vehicle-treated mice (black line) and vorinostat-treated mice (dashed line) are shown. (*g*) The histograms show the cell cycle profiles of E$\mu$-myc/Bcl-2 lymphomas harvested from the lymph nodes of transplanted C57BL/6 mice after 12-h treatment with vehicle (*Upper*) or vorinostat (*Lower*). (*h*) Treatment of E$\mu$-myc/Bcl-2 lymphomas commenced on day 6 after tumor injection and terminated on day 13. Kaplan–Meier survival curves of vehicle-treated mice (black line) and vorinostat-treated mice (dashed line) are shown. *, $P < 0.05$; **, $P = 0.13$.

survival vehicle = 18 days, median survival vorinostat = 34 days, $P = 0.0005$) and vorinostat induced a statistically significant reduction of WBC counts after 1 week of treatment (Fig. 2*e*). Autopsy of vehicle-treated mice revealed disseminated disease throughout the lymphoid system with enlarged lymph nodes and splenomegaly. Vorinostat-treated mice autopsied at the same time displayed no overt signs of lymphoma (SI Fig. 10). Similar vorinostat-mediated effects on lymphoma survival, WBC counts, and therapeutic outcome were observed by using two additional, independently derived E$\mu$-myc lymphomas (SI Fig. 11 *a* and *b*). Although mice succumbed to disease after cessation of vorinostat treatment, *in vitro* assays using lymphomas from relapsed mice showed no evidence that these cells were less sensitive to vorinostat than parental cells that had never been exposed to vorinostat (data not shown).

**Vorinostat Therapy Is p53-Independent but Abrogated by Overexpression of Bcl-2.** E$\mu$-myc/p53$^{-/-}$ tumors were sensitive to vorinostat *in vivo* (Fig. 3 *a* and *b*); however, these cells were relatively resistant to the DNA-damaging agent etoposide (Fig. 3*a Inset*). A robust therapeutic response was achieved by using vorinostat against E$\mu$-myc/p53$^{-/-}$ lymphomas [Fig. 3*c* (median survival vehicle = 11.5 days, median survival vorinostat = 28.5 days, $P < 0.0001$) and SI Fig. 12 ($n$ = three independently derived lymphomas analyzed] that was preceded by a significant decrease in WBC counts to normal levels (Fig. 3*d*).

Consistent with our *in vitro* data (Fig. 1*b* and SI Fig. 8), vorinostat was unable to kill Bcl-2 overexpressing E$\mu$-myc lymphomas *in vivo* (Fig. 3 *e* and *f*) but did arrest cells in the $G_1$ (Fig. 3*g*). The loss of vorinostat-induced apoptosis translated into a dramatic reduction of therapeutic efficacy [Fig. 3*h* (median survival vehicle = 10 days, median survival vorinostat = 13 days, $P < 0.0001$) and SI Fig. 13 ($n$ = two independent lymphomas analyzed], and vorinostat did not cause a decline in WBC counts (Fig. 3*i*). Similar results were obtained by using E$\mu$-myc lymphomas overexpressing Bcl-$X_L$ (SI Fig. 14). Taken together, these data indicate that, in myc-driven murine lymphomas, apoptosis mediated by the intrinsic apoptotic pathway is critical for the therapeutic response to vorinostat.

**Role of the Extrinsic Cell Death Pathway and Identification of the BH3-Only Proteins Bim and Bid as Targets in Vorinostat-Mediated Lymphoma Therapy.** In acute myeloid leukemias tumor cell-selective up-regulation of death receptors (i.e., DR5, Fas) and their cognate ligands [i.e., tumor necrosis factor-related apoptosis-inducing ligand (TRAIL), Fas ligand (FasL)] are reported to play an important role in the therapeutic response to HDACi (18, 19). To evaluate the role of TRAIL in mediating the therapeutic activity of vorinostat, we generated E$\mu$-myc/

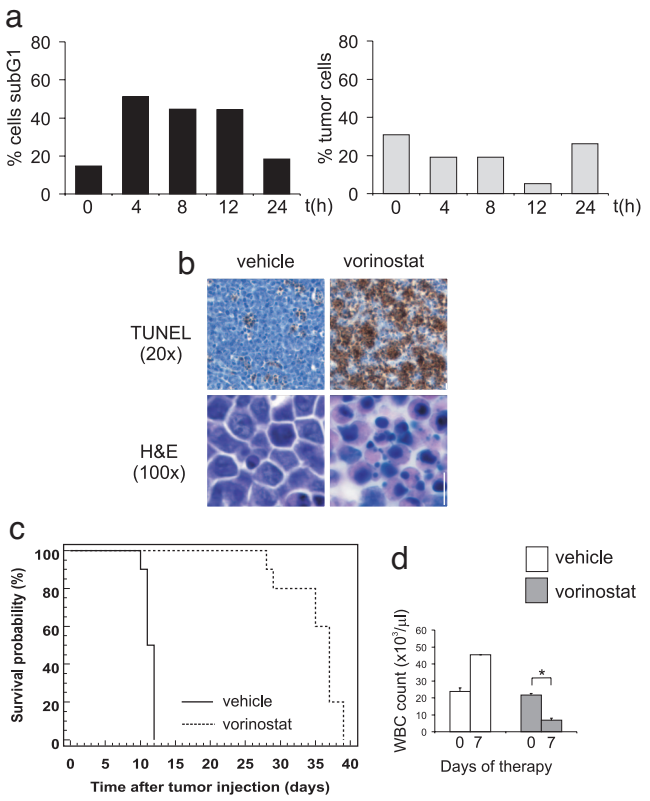


**Fig. 4.** Antitumor efficacy of vorinostat is unaffected by inhibition of death receptor signaling through CrmA overexpression. Eμ-myc/CrmA lymphomas were transplanted into C57BL/6 mice and vorinostat-induced apoptosis *in vivo* (*a* and *b*), therapy (*c*), and depletion of WBC counts (*d*) were assessed as in Fig. 2. Treatment commenced on day 6 after tumor injection and terminated on day 34. Kaplan–Meier survival curves of vehicle-treated mice (black line) and vorinostat-treated mice (dashed line) are shown. *, $P < 0.05$.

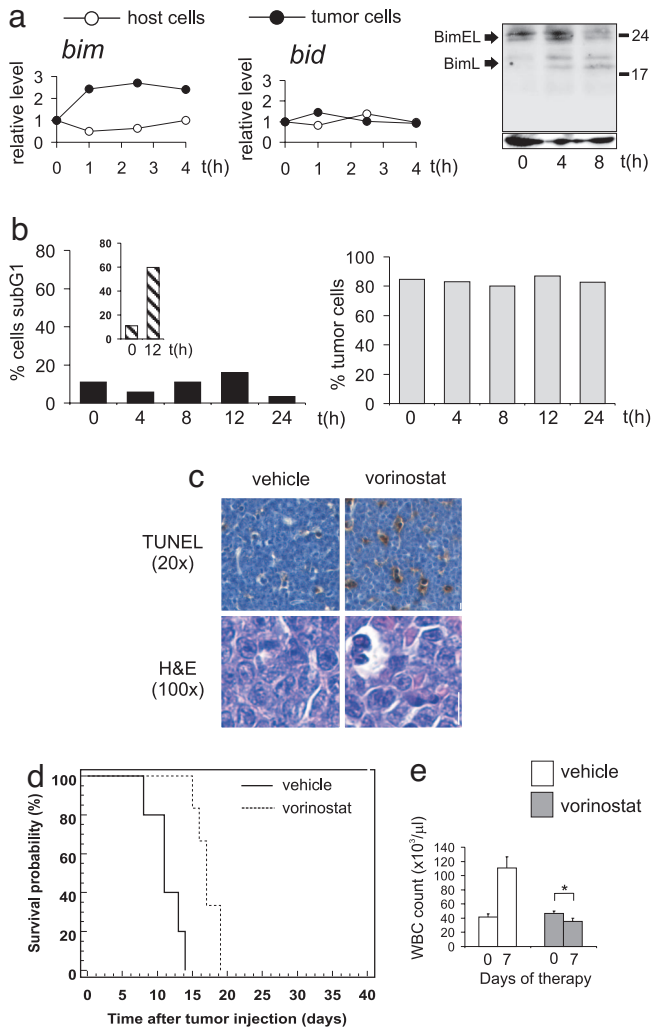


**Fig. 5.** Bim is a previously unrecognized target for HDACi *in vivo*. (*a*) Up-regulation of Bim mRNA and protein by vorinostat. (*Left*) Levels of *bim* and *bid* mRNA were measured by quantitative real-time PCR in the lymphoma cells and in nontumor cells, respectively. Two independent sets of mice were examined and relative induction of mRNA levels are shown for one representative cohort. (*Right*) Eμ-myc lymphomas were transplanted into C57BL/6 mice, which were subsequently treated with 200 mg/kg vorinostat. Lymph nodes were harvested after the indicated time points, and Western blotting was performed by using an anti-murine Bim antibody. Blots were stripped and reprobed with an anti-Hsp70 antibody to ensure equivalent protein loading. Eμ-myc/Bim$^{-/-}$ lymphomas were transplanted into C57BL/6 mice, and vorinostat-induced apoptosis *in vivo* (*b* and *c*), therapy (*d*), and suppression of WBC counts (e) were assessed as in Fig. 2. Treatment commenced on day 9 after tumor injection and terminated on day 34. Kaplan-Meier survival curves of vehicle-treated mice (black line) and vorinostat-treated mice (dashed line) are shown. *, $P = 0.058$.

TRAIL$^{-/-}$ lymphomas. These cells were sensitive to vorinostat-induced apoptosis *in vivo*, and the therapeutic efficacy against the Eμ-myc/TRAIL$^{-/-}$ lymphomas was similar to that seen against Eμ-myc and Eμ-myc/p53$^{-/-}$ tumors (SI Fig. 15).

The role of extrinsic apoptotic pathway in vorinostat-mediated tumor cell death, was further evaluated in lymphoma cells that overexpress the viral serpin CrmA, which effectively blocks death receptor signaling through inhibition of caspase-8 and -10 (20). Eμ-myc/CrmA lymphomas were sensitive to vorinostat *in vivo* (Fig. 4 *a* and *b*) and displayed therapeutic responsiveness [Fig. 4*c* (median survival vehicle = 11.5 days, median survival vorinostat = 37 days, $P < 0.0001$) and SI Fig. 16] and decreased WBC counts (Fig. 4*d*) similar to that seen using Eμ-myc, Eμ-myc/p53$^{-/-}$, and Eμ-myc/TRAIL$^{-/-}$ lymphomas. Taken together, these data indicate that, in contrast to the reported role of death receptor signaling in mediating HDACi-induced death of myeloid leukemia cells (18, 19), there is no evidence to support a role for this pathway in vorinostat-induced apoptosis and therapy of c-myc-driven lymphomas.

To identify the molecular events in the intrinsic apoptotic pathway necessary for vorinostat-mediated apoptosis of Eμ-myc lymphomas, we performed genotype-response analyses using lymphomas lacking the proapoptotic BH3-only proteins Bid and Bim, which can act as upstream inducers of Bcl-2-dependent mitochondrial apoptosis (21). The proapoptotic BH3-only molecule Bid is activated upon HDACi treatment of cultured human leukemia CCRF-CEM cells (3). Treatment of Eμ-myc lymphomas with vorinostat *in vivo* resulted in cleavage of Bid in a tumor cell-specific and time-dependent manner (SI Fig. 17*a*). We generated Eμ-myc/Bid$^{-/-}$ lymphoma cells to assess the importance of Bid in mediating vorinostat-induced apoptosis. Bid deficiency suppressed the *in vivo* apoptotic activity of vorinostat (SI Fig. 17 *b* and *c*), and loss of Bid attenuated the therapeutic effect of vorinostat with early tumor relapse evident while mice were still receiving therapy (SI Fig. 17). Moreover, vorinostat failed to significantly decrease WBC numbers in these mice.

When we administered vorinostat to Eμ-myc lymphoma-bearing mice, we noted that *bim*, but not *bid* mRNA was induced specifically in lymphoma cells, but not in untransformed lymphocytes (Fig. 5*a*) and the $Bim_L$ protein isoform was up-regulated by vorinostat *in vivo*. (Fig. 5*a Right*). Bim deficiency

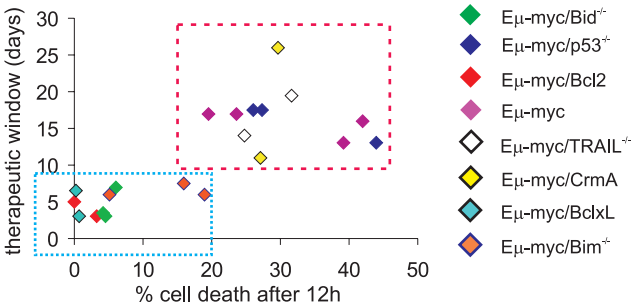


**Fig. 6.** Apoptotic sensitivity to vorinostat *in vivo* correlates with therapeutic outcome. Sensitivity of lymphomas in the IVA assay correlates with therapeutic outcome. Specific cell death [(percent cell death after 12 h of vorinostat) − (percent cell death at 0 h)] was plotted against the therapeutic window [(median survival vorinostat cohort) − (median survival control cohort)]. Bcl-2- and Bcl-$X_L$-overexpressing Bid$^{-/-}$ and Bim$^{-/-}$ lymphomas show low *in vivo* sensitivity to vorinostat, reduced responsiveness in therapy experiments, and form a ''resistance'' cluster (blue box). Eμ-myc, Eμ-myc/p53$^{-/-}$, Eμ-myc/TRAIL$^{-/-}$, and Eμ-myc/CrmA lymphomas were sensitive to vorinostat *in vivo* and formed a sensitive cluster (red box). The color of the diamonds corresponds to different genotypes, as outlined to the right. Statistical analysis: Mean specific cell death-resistant cluster = 5.9%; 95% confidence interval (CI) = 1.3–10.6%. Mean specific cell death in sensitive cluster = 30.4%; 95% CI = 25.1–35.8; $P < 0.0001$. Mean therapeutic window resistant cluster = 5.1 days; 95% CI = 3.8–6.3. Mean therapeutic window sensitive cluster = 16.5 days; 95% CI = 13.8–19.2; $P < 0.0001$.

severely decreased responsiveness to vorinostat as shown by *in vivo* apoptosis assay (IVA) and TUNEL analyses (Fig. 5 *b* and *c*). In contrast, the apoptotic response to Etoposide was not altered (compare Fig. 2*a Inset* with Fig. 5*b Inset*). Mice bearing Eμ-myc/Bim$^{-/-}$ lymphomas relapsed early during vorinostat therapy [Fig. 5*d* (median survival vehicle = 11 days, median survival vorinostat = 17 days, $P = 0.0007$) and SI Fig. 18 ($n$ = three independently derived lymphomas analyzed)] and WBC counts were not significantly reduced (Fig. 5*e*). Taken together, these data show that proapoptotic signaling by the BH3-only proteins Bim and Bid plays an important role in vorinostat-mediated lymphoma therapy.

***In Vivo* Apoptotic Response Predicts Therapeutic Outcome.** We compared therapeutic outcome with sensitivity to vorinostat-induced apoptosis for independently derived lymphomas of multiple genotypes. A statistically significant correlation ($R = 0.76$ for linear regression) was observed between ''specific death'' as determined by *in vivo* apoptosis assays and ''survival benefit'' [median survival (vorinostat-treated mice) − median survival (vehicle-treated mice)] (Fig. 6). Lymphomas with overexpression of Bcl-2, Bcl-$X_L$, or deletion of Bid or Bim formed a ''therapy-resistant'' cluster (Fig. 6, blue box). In contrast, unmodified Eμ-myc lymphomas and those compound mutant lymphomas with deactivated extrinsic apoptotic pathways or deletion of p53 grouped together in a ''therapy-sensitive'' cluster (Fig. 6, red box). Robust suppression of WBC counts after 1 week of vorinostat therapy was only observed in Eμ-myc, Eμ-myc/p53$^{-/-}$, Eμ-myc/TRAIL$^{-/-}$, and Eμ-myc/CrmA lymphomas, but not in lymphomas with defects in apoptosis mediated by the intrinsic pathway (SI Fig. 19*a*). Indeed, all but one lymphoma of the resistant genotypes (Eμ-myc/Bcl-2, Eμ-myc/Bcl-$X_L$, Eμ-myc Bid$^{-/-}$, Eμ-myc Bim$^{-/-}$) fatally relapsed within 1 week after onset of treatment, whereas none of the other genotypes did so, and contingency analysis revealed high statistical significance (SI Fig. 19*b*).

## Discussion

HDACi can elicit diverse biological responses such as induction of cellular differentiation, suppression of cell proliferation, apoptosis, inhibition of angiogenesis, and modulation of immune responses (2). The molecular pathways of HDACi-induced apoptosis *in vivo* are not fully elucidated. Herein, we used the Eμ-myc transgenic mouse model of B cell lymphoma to systematically assess genotype-response relationships in a series of lymphomas with defined genetic alterations in apoptotic pathways. We found a direct link between HDACi-induced apoptosis and therapeutic efficacy. Vorinostat engaged the intrinsic apoptotic pathway in a p53-independent manner. The apoptotic and therapeutic activities of vorinostat were attenuated in cells devoid of the proapoptotic BH3-only Bcl-2 family proteins Bid or Bim. The death receptor pathway was not required for the apoptotic or therapeutic activities of the HDACi vorinostat. Furthermore, our studies show that, for Eμ-myc lymphomas, the therapeutic efficacy of vorinostat could be predicted on the basis of the short-term *in vivo* responsiveness of lymphoma cells to vorinostat as determined by our IVA assay and reduction in WBC numbers. Vorinostat induced equivalent histone hyperacetylation in resistant and sensitive Eμ-myc lymphomas, indicating that the inhibition of vorinostat-mediated apoptosis and therapy occurs downstream of histone hyperacetylation.

We identified the BH3-only proteins Bid and Bim as important regulators of vorinostat-mediated apoptosis and therapy. Here, we report previously unrecognized evidence that vorinostat treatment up-regulates Bim mRNA and protein *in vivo*, and our results are in agreement with an *in vitro* study that showed that decreasing expression of Bim by siRNA suppressed the apoptotic effect of vorinostat (22). *Bim* expression can be regulated by transcription factors such as Foxo3a (23) and E2F1 (22). Addition of HDACi augments the transcriptional activation Bim by these factors.

We and others have shown that Bid is cleaved and activated in tumor cell lines treated with HDACi *in vitro* (3, 4, 6, 24), and we demonstrate herein that Bid is cleaved in a tumor cell-selective manner *in vivo* after administration of vorinostat. *Bid* is clearly important for the apoptotic and therapeutic activity of vorinostat. This effect appears to be selective for vorinostat as Eμ-myc/Bid$^{-/-}$ lymphomas remain fully sensitive to other chemotherapeutic drugs such as etoposide. We have yet to identify the protease(s) responsible for vorinostat-induced cleavage and activation of Bid. We have shown that the caspase inhibitor zVAD-fmk, which can suppress vorinostat-induced cleavage of poly(ADP-ribose) polymerase (PARP), does not affect this process (3, 4). Studies with various transformed cells, including our preliminary data using Eμ-myc/Puma$^{-/-}$ lymphoma cells (data not shown), indicate that not all BH3-only proteins are likely to be involved in the apoptotic response to vorinostat (3, 6, 7, 9, 24).

HDACi have shown promise in early-phase clinical trials for the treatment of hematological malignancies, and, in a phase IIb open-label study, 24% of cutaneous T cell lymphoma (CTCL) patients who had failed conventional therapies had a complete or partial response to vorinostat as a single agent (25). Vorinostat is the first HDACi to receive Food and Drug Administration approval as an anticancer drug for the treatment of CTCL (12). Our data provide insight into the molecular events that underpin vorinostat-induced apoptosis and identify lesions within specific apoptotic pathways that lead to resistance to vorinostat. Specifically, overexpression of Bcl-2 or Bcl-$X_L$ or the loss of expression of Bid or Bim abrogate the effects of vorinostat. Human leukemias and lymphomas commonly overexpress prosurvival Bcl-2 proteins as do certain solid tumors (13). In addition, the BH3-only proteins Bim and Bid show tumor-suppressor function in certain contexts (26, 27), and inactivating mutations or loss of expression in human cancer samples have been reported (28–30). On the basis of our findings, the significance of the expression and/or functional status of prosurvival Bcl-2 proteins and certain proapoptotic BH3-only proteins

across a range of hematological and solid tumors should be studied in greater detail.

## Materials and Methods

**Eμ-myc Lymphomas.** Lymphomas were isolated from Eμ-myc or Eμ-myc/p53$^{-/-}$ transgenic mice (11). Eμ-myc/Bcl-2, Eμ-myc/Bcl-$X_L$, and Eμ-myc/CrmA lymphomas were engineered by retroviral transduction of freshly isolated lymphoma cells and the generation of Bid$^{-/-}$, Bim$^{-/-}$, and TRAIL$^{-/-}$ Eμ-myc lymphomas are detailed in *SI Methods*.

***In Vitro* Cell Death Analysis.** Eμ-myc lymphoma cells ($2–5 \times 10^5$) were incubated in the presence of the indicated compounds for 20 h, and cell viability was measured by trypan blue exclusion assay (3) or propidium iodide (PI) (31) MOMP was analyzed by using tetramethyl-rhodamine ethyl ester (TMRE) (31). Caspase activity was measured as described in refs. 7 and 8. Cell cycle analysis using PI staining was performed (4). IVA is detailed in *SI Methods*.

**Mice.** For IVA and therapy studies, 6- to 8-week-old C57BL/6 mice were used. The Peter MacCallum Cancer Centre Animal Ethics Committee approved all mouse protocols used in this study. PCR-based genotyping and Western blot analysis were used to validate lymphoma genotypes (data not shown).

**Extraction of Histones and Western Blotting.** Histone extracts and whole-cell lysates were prepared as described in ref. 4. Proteins were separated by SDS/10% polyacrylamide gel electrophoresis, and Western blotting was performed (4).

**Therapy Experiments.** C57BL/6 mice were injected i.v. with $5 \times 10^5$ Eμ-myc lymphoma cells of the indicated genotypes. Peripheral WBC counts were monitored, and therapy commenced when counts exceeded $13 \times 10^3$ per microliter (Sysmex Hematology Analyzer K-1000; Sysmex, Malberg, Germany). Vorinostat was administered at 200 mg/kg i.p. for 7 days, followed by i.p. vorinostat for 14–21 days at 150 mg/kg. Control mice received the corresponding amount of DMSO. Cohorts consisted of 8–11 mice each and two to three independently derived lymphomas per genotype. Peripheral WBC counts and body weights were recorded weekly. For analysis of therapeutic efficacy, tumor-induced mortality "events" were recorded. Histology and TUNEL staining were performed as detailed in the *SI Methods*.

**Statistics.** Kaplan–Meier analysis was performed and comparisons were made using the log-rank (Mantel–Cox) test (MedCalc software, version 8.0.2.0; MedCalc, Mariakerke, Belgium). *P* values were calculated by using a two-way *t* test. Ninety-five-percent confidence intervals were calculated by using MedCalc software. Contingency analysis was performed by using the StatPages online tool.

We thank Rachel Cameron and Daniela Cardozo for assistance with mouse experimentation; Nathalie Thompson for help with statistical analysis; Chris Clarke, Jane Oliaro, Ilia Voskoboinik, and Nigel Waterhouse for critical discussion; David Huang, Andreas Strasser, Jerry Adams, Suzanne Cory, and Alan Harris (all at the Walter and Eliza Hall Institute) for Eμ-*myc* mice and Eμ-*myc*/*bim*$^{-/-}$ lymphomas; Stan Korsmeyer (Dana–Farber Cancer Institute, Boston, MA) for *bid*$^{-/-}$ mice; and Jacques Peschon (Immunex Corporation, Seattle, WA) for *trail*$^{-/-}$ mice. Depsipeptide was provided by Gloucester Pharmaceuticals (Cambridge, MA). R.W.J. is a Pfizer Australia Research Fellow and is supported by Australian National Health and Medical Research Council Program Grant 251608, the Cancer Council Victoria, the Leukemia Foundation of Australia, and a Merck and Co. research grant. A.J.F. is supported by the Cancer Research Institute Predoctoral Emphasis Pathway in Tumor Immunology. M.J.S. is a Senior Principal Research Fellow of the Australian National Health and Medical Research Council. C.L.S. is supported by fellowships from the Seligson Foundation and the Leukemia and Lymphoma Society and Australian National Health and Medical Research Council Grant 461261. P.A.M. is supported by National Institutes of Health Grant P30CA08748-41, the David H. Koch Foundation, and the Experimental Therapeutics Center at the Memorial Sloan–Kettering Cancer Center. Work from the Walter and Eliza Hall Institute was supported by the Australian National Health and Medical Research Council Program Grant 257502, U.S. National Cancer Institute Grant CA43540, and Leukemia and Lymphoma Society Specialized Center of Research Grant 7015-02.

1. Lindemann RK, Gabrielli B, Johnstone RW (2004) *Cell Cycle* 3:779–788.
2. Bolden JE, Peart MJ, Johnstone RW (2006) *Nat Rev Drug Discov* 5:769–784.
3. Ruefli AA, Ausserlechner MJ, Bernhard D, Sutton VR, Tainton KM, Kofler R, Smyth MJ, Johnstone RW (2001) *Proc Natl Acad Sci USA* 98:10833–10838.
4. Peart MJ, Tainton KM, Ruefli AA, Dear AE, Sedelies KA, O'Reilly LA, Waterhouse NJ, Trapani JA, Johnstone RW (2003) *Cancer Res* 63:4460–4471.
5. Rosato RR, Almenara JA, Grant S (2003) *Cancer Res* 63:3637–3645.
6. Mitsiades N, Mitsiades CS, Richardson PG, McMullan C, Poulaki V, Fanourakis G, Schlossman R, Chauhan D, Munshi NC, Hideshima T, *et al.* (2003) *Blood* 101:4055–4062.
7. Xu W, Ngo L, Perez G, Dokmanovic M, Marks PA (2006) *Proc Natl Acad Sci USA* 103:15540–15545.
8. Ruefli AA, Bernhard D, Tainton KM, Kofler R, Smyth MJ, Johnstone RW (2002) *Int J Cancer* 99:292–298.
9. Minucci S, Pelicci PG (2006) *Nat Rev Cancer* 6:38–51.
10. Schmitt CA, Rosenthal CT, Lowe SW (2000) *Nat Med* 6:1029–1035.
11. Schmitt CA, Fridman JS, Yang M, Baranov E, Hoffman RM, Lowe SW (2002) *Cancer Cell* 1:289–298.
12. Marks PA, Breslow R (2007) *Nat Biotechnol* 25:84–90.
13. Johnstone RW, Ruefli AA, Lowe SW (2002) *Cell* 108:153–164.
14. Xu Y (2003) *Cell Death Differ* 10:400–403.
15. Gu W, Roeder RG (1997) *Cell* 90:595–606.
16. Terui T, Murakami K, Takimoto R, Takahashi M, Takada K, Murakami T, Minami S, Matsunaga T, Takayama T, Kato J, Niitsu Y (2003) *Cancer Res* 63:8948–8954.
17. Adams JM, Harris AW, Pinkert CA, Corcoran LM, Alexander WS, Cory S, Palmiter RD, Brinster RL (1985) *Nature* 318:533–538.
18. Insinga A, Monestiroli S, Ronzoni S, Gelmetti V, Marchesi F, Viale A, Altucci L, Nervi C, Minucci S, Pelicci PG (2005) *Nat Med* 11:71–76.
19. Nebbioso A, Clarke N, Voltz E, Germain E, Ambrosino C, Bontempo P, Alvarez R, Schiavone EM, Ferrara F, Bresciani F, *et al.* (2005) *Nat Med* 11:77–84.
20. Garcia-Calvo M, Peterson EP, Leiting B, Ruel R, Nicholson DW, Thornberry NA (1998) *J Biol Chem* 273:32608–32613.
21. Willis SN, Adams JM (2005) *Curr Opin Cell Biol* 17:617–625.
22. Zhao Y, Tan J, Zhuang L, Jiang X, Liu ET, Yu Q (2005) *Proc Natl Acad Sci USA* 102:16090–16095.
23. Brunet A, Sweeney LB, Sturgill JF, Chua KF, Greer PL, Lin Y, Tran H, Ross SE, Mostoslavsky R, Cohen HY, *et al.* (2004) *Science* 303:2011–2015.
24. Rosato RR, Almenara JA, Dai Y, Grant S (2003) *Mol Cancer Ther* 2:1273–1284.
25. Duvic M, Talpur R, Ni X, Zhang C, Hazarika P, Kelly C, Chiao JH, Reilly JF, Ricker JL, Richon VM, Frankel SR (2007) *Blood* 109:31–39.
26. Egle A, Harris AW, Bouillet P, Cory S (2004) *Proc Natl Acad Sci USA* 101:6164–6169.
27. Zinkel SS, Ong CC, Ferguson DO, Iwasaki H, Akashi K, Bronson RT, Kutok JL, Alt FW, Korsmeyer SJ (2003) *Genes Dev* 17:229–239.
28. Smith L, Berrieman HK, O'Kane SL, Campbell A, Maraveyas A, Cawkwell L (2006) *Oncol Res* 15:441–444.
29. Lee JH, Soung YH, Lee JW, Park WS, Kim SY, Cho YG, Kim CJ, Seo SH, Kim HS, Nam SW, *et al.* (2004) *J Pathol* 202:439–445.
30. Mestre-Escorihuela C, Rubio-Moscardo F, Richter JA, Siebert R, Climent J, Fresquet V, Beltran E, Agirre X, Marugan I, Marin M, *et al.* (2006) *Blood*
31. Essmann F, Engels IH, Totzke G, Schulze-Osthoff K, Janicke RU (2004) *Cancer Res* 64:7065–7072.